

## Manipulation of magnetic skyrmions with a scanning tunneling microscope

R. Wieser, R. Shindou, and X. C. Xie

*International Center for Quantum Materials, Peking University, Beijing 100871, China  
and Collaborative Innovation Center of Quantum Matter, Beijing 100871, China*

(Received 21 September 2016; revised manuscript received 17 January 2017; published 17 February 2017)

The dynamics of a single magnetic skyrmion in an atomic spin system under the influence of a scanning tunneling microscope is investigated by computer simulations solving the Landau-Lifshitz-Gilbert equation. Two possible scenarios are described: manipulation with aid of a spin-polarized tunneling current and by an electric field created by the scanning tunneling microscope. The dynamics during the creation and annihilation process is studied and the possibility to move single skyrmions is showed.

DOI: [10.1103/PhysRevB.95.064417](https://doi.org/10.1103/PhysRevB.95.064417)

Due to the possibility to use magnetic skyrmions as potential candidates for data storage [1–3], for logic devices [4], or as a skyrmion transistor [5], magnetic skyrmions have been intensively studied during the last period of time. The idea to use local differences in the magnetic structure is not new: Bubble domains in thin film structures [6], magnetic domain walls in nanowires driven by an electric current [7], and magnetic vortices [8,9] have been considered as candidates for data storage and/or logic devices. However, due to the stability as a result of the topology (topological protected) and the dimension (a few nanometer) magnetic skyrmions are promising candidates for future spintronic devices.

Furthermore, magnetic skyrmions appear in thin film systems on the microscopic [10–12] but also on the atomic length scale [13,14]. Current investigation mostly focus on magnetic skyrmions at the microscopic length scale. The reason can be found in the possibility to observe these skyrmions at room temperature and with several experimental techniques like, e.g., magnetic transmission x-ray microscopy [11] or magneto-optical Kerr effect microscopy [10,15]. The investigation of magnetic skyrmions at the atomic length scale is more challenging. Here a scanning tunneling microscope (STM) and low temperatures ( $T \approx 4$  K) are needed. On the other hand, the technological goal is to reduce the size which is needed to store information. Therefore, magnetic skyrmions on the atomic length scale can be seen as the next step after realizing skyrmion devices on the microscopic scale.

The first step toward this direction has been already done. Recent experiments have shown that it is possible to switch magnetic skyrmions on the atomic length scale with aid of an STM [13,16]. Within these publications two different methods to manipulate magnetic skyrmions will be described: (1) creating and annihilating skyrmions with spin-polarized tunnel currents and (2) using electric fields. While for the first experiment a magnetized STM tip is needed, this is not the case for the switching process using electric fields. Therefore, the manipulation using electric fields is preferable. However, the problematic point in both experimental situations is the time resolution. The time resolution of a conventional scanning tunneling microscope is not high enough to investigate the dynamics during the experiment. Therefore, spin dynamics simulations are a perfect way to investigate the dynamics and to get deeper insights into the physics of skyrmions.

The theoretical publications [17,18] discuss the ground state configuration, the energy barrier between the ferromagnetic and the skyrmion state, and give an idea about the dynamics. However, these publications do not describe the creation or annihilation processes using spin-polarized tunneling currents or electric fields. This information will be given in this paper which provides a description of the switching dynamics using STM in both cases, spin polarized with tunneling currents and not spin polarized using electric fields. Furthermore, the possibility to move a single skyrmion with aid of an STM and without disturbing the surrounding skyrmions is demonstrated. The results of the performed spin dynamics simulations are described in this paper and also given as videos attached as Supplemental Materials [19].

The investigated system is a spin system with a triangular lattice on the atomic length scale and with lattice constant  $a \approx 2.7$  Å. The system is analog to the double layer Pd/Fe on Ir(111) described in [17,18]. The lateral dimension of the film is  $L_x \times L_y = 26.325$  nm  $\times$  45.6 nm (39204 spins) and the magnetic properties of the system are well described by the following Hamiltonian:

$$\mathcal{H} = -J \sum_{\langle n,m \rangle} \mathbf{S}_n \cdot \mathbf{S}_m - \sum_{\langle n,m \rangle} \mathcal{D}_{nm} \cdot (\mathbf{S}_n \times \mathbf{S}_m) - \mu_S B_z \sum_n S_n^z - D_z \sum_n (S_n^z)^2.$$

The first two terms are the ferromagnetic exchange and Dzyaloshinsky-Moriya interaction (DMI) where  $J = 7$  meV and  $|\mathcal{D}_{nm}| = 2.2$  meV. The Dzyaloshinsky-Moriya vectors  $\mathcal{D}_{nm}$  are oriented in-plane (film plane) perpendicular to the lattice vector  $\mathbf{r}_{nm} = \mathbf{r}_m - \mathbf{r}_n$  pointing from lattice site  $n$  to  $m$ . The third term describes the influence of an external magnetic field perpendicular to the film plane in  $z$  direction and the fourth term an uniaxial anisotropy with easy axis in  $\pm z$  direction and  $D_z = 0.7$  meV.

In the following an external field of  $B_z = 3.0$  T is assumed which provides stable magnetic skyrmions which due to the in-plane orientation of  $\mathcal{D}_{nm}$  show a hedgehog structure with magnetic moments pointing to the center of the skyrmion. The skyrmionic structure as well as the color coding of the pictures are given in Fig. 1. All figures have the same camera position and therefore the same color coding even if the focus is changed. The diameter of the skyrmion depends on the

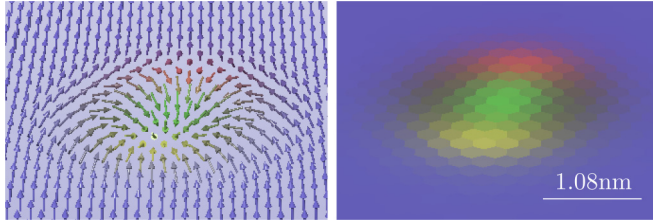


FIG. 1. Single magnetic skyrmion at  $B_z = 3$  T. Left: Triangular lattice with Néel type magnetic skyrmion. Right: Corresponding continuum picture.

strength of the external field: Corresponding to  $B_z = 3.0$  T the found skyrmion diameter is  $d \approx 3.24$  nm.

The dynamics of the system is described by the Landau-Lifshitz-Gilbert (LLG) equation with additional spin transfer torques:

$$\frac{\partial \mathbf{S}_n}{\partial t} = -\frac{\gamma}{(1 + \alpha^2)\mu_S} \mathbf{S}_n \times [\mathbf{H}_n + \alpha(\mathbf{S}_n \times \mathbf{H}_n)] - \mathbf{S}_n \times [\mathcal{A}\mathbf{T}_n + \mathcal{B}(\mathbf{S}_n \times \mathbf{T}_n)].$$

The first and second term are the precessional and relaxation term of the conventional LLG equation with the effective field  $\mathbf{H}_n = -\partial\mathcal{H}/\partial\mathbf{S}_n + \xi_n$ , where  $\xi_n$  is white noise. The simulations have been performed at  $T = 4$  K plus an additional Joule heating of 0.5 K within a spot (radius  $r_0 \approx 0.88$  nm) underneath the tip and for comparison without temperature ( $T = 0$  K). All presented figures, except Fig. 4, show results of the simulations at zero temperature. Figure 4 shows two snapshots of the nonzero temperature simulations. The videos are available for  $T = 0$  K and  $T = 4$  K, respectively.

The other parameters in the first two terms of the LLG equation are the gyromagnetic ratio  $\gamma = 1.76 \times 10^{11} \frac{1}{T_s}$ , the magnetic moment  $\mu_S = 3.3 \mu_B$  in Bohr magneton  $\mu_B$ , and the dimensionless Gilbert damping constant  $\alpha = 0.02$ . The third and fourth term are spin transfer torques describing the influence of a spin-polarized current. These terms have been modified to describe the tunnel current of a spin-polarized scanning tunneling microscope:  $\mathcal{A} = 0.05$  and  $\mathcal{B} = 1.0$  have been assumed. The model which describes the local strength of the current is the Tersoff-Hamann model [20,21] which leads to

$$\mathbf{T}_n = I_0 e^{-2\kappa \sqrt{(x_n - x_{\text{tip}})^2 + (y_n - y_{\text{tip}})^2 + h^2}} \mathbf{P},$$

where  $\mathbf{P} = \pm \hat{z}$  is the tip polarization,  $I_0$  is the strength of the current,  $\kappa = 0.93 \times 10^{10}$  1/m is related to the work function of the tip, and  $\mathbf{r}_{\text{tip}}(t) = [x_{\text{tip}}(t), y_{\text{tip}}(t), h]^T$  is the tip position, which is time dependent. The tip-sample distance  $h = 5.4 \text{ \AA}$  has been assumed to be constant.  $\mathbf{r}_n = (x_n, y_n, 0)$  is the position vector within the lattice. Figure 2 provides a sequence of pictures showing the creation and annihilation of a magnetic skyrmion with a spin-polarized tunnel current. The starting configuration with a ferromagnetic orientation of the magnetic moments underneath the STM tip is given in Fig. 2(a). After a current pulse of 8 ps with  $I_0^{\text{max}} = 1.27 \times 10^{19}$  1/s a skyrmion is created. In total the creating process takes just a few picoseconds. Figures 2(b) and 2(c) show two moments during the creation of the skyrmion. The process starts with the reversal of the magnetic moments underneath the magnetic tip

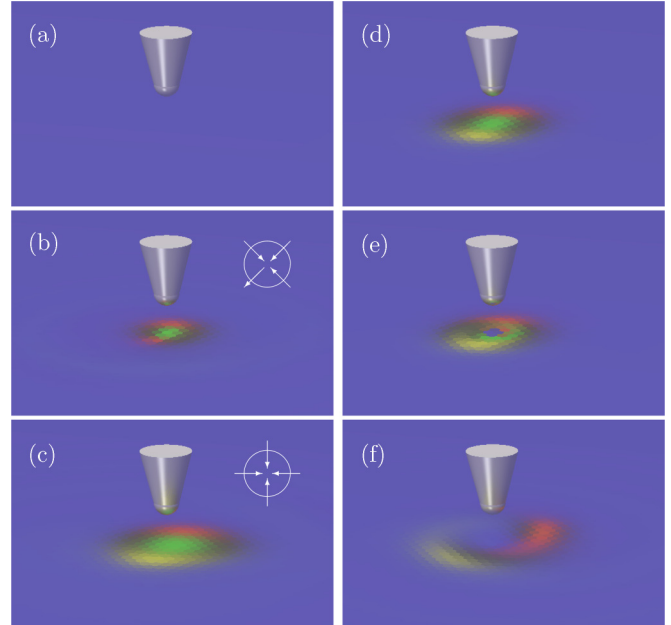


FIG. 2. Creation and annihilation of a skyrmion with current pulses from a spin-polarized STM tip. Left column: Creation with tip polarization  $\mathbf{P} = -\hat{z}$ . Right column: Annihilation with tip polarization  $\mathbf{P} = +\hat{z}$ . The pictograms show schematic the in-plane orientation of the magnetization.

forced by the tunnel current. The tip polarization  $\mathbf{P}$  is assumed to be in  $-z$  direction which is opposite to the orientation of the ferromagnetically aligned magnetic moments. After a short moment a bubble domain with opposite magnetization in the center is created. The in-plane magnetization (domain wall) of the bubble domain shows at approximately 3/4 of the circumference to the center but at 1/4 to the outside [see pictogram in Fig. 2(b)]. Calculating the winding number  $w$  [22], also called skyrmion number, for the bubble domain one finds  $w = 0$ . This value is similar to the winding number of the surrounding ferromagnet. Therefore, this configuration is not stable. However, the simulations show that the bubble domain is just temporary and becomes a magnetic skyrmion which is stable due to  $w = 1$ . The created skyrmion has an overpassed size at the beginning. During the shrinking to normal size the skyrmion shows first nonlinear excitations: fuzzy oscillation which becomes a breathing mode [23–25] with frequency  $f \approx 100$  GHz. The final configuration is the magnetic skyrmion shown in Fig. 2(d).

Another current pulse with opposite tip polarization can be used to annihilate the skyrmion. Figures 2(e) and 2(f) show two snapshots of the destruction process. While during the skyrmion creation the tunneling current creates a small spot of opposite magnetization, which becomes the center of the skyrmion, in the case of the annihilation process the tunnel current orients all spins underneath the tip parallel to the surrounding ferromagnet. This means the tunnel current destroys the center of the skyrmion (core) and therefore the skyrmion. The annihilation process starts from the inside and releases energy when the skyrmion gets destroyed. Therefore, the annihilation process appears like an explosion where a concentric shockwave starting underneath the tip and exciting

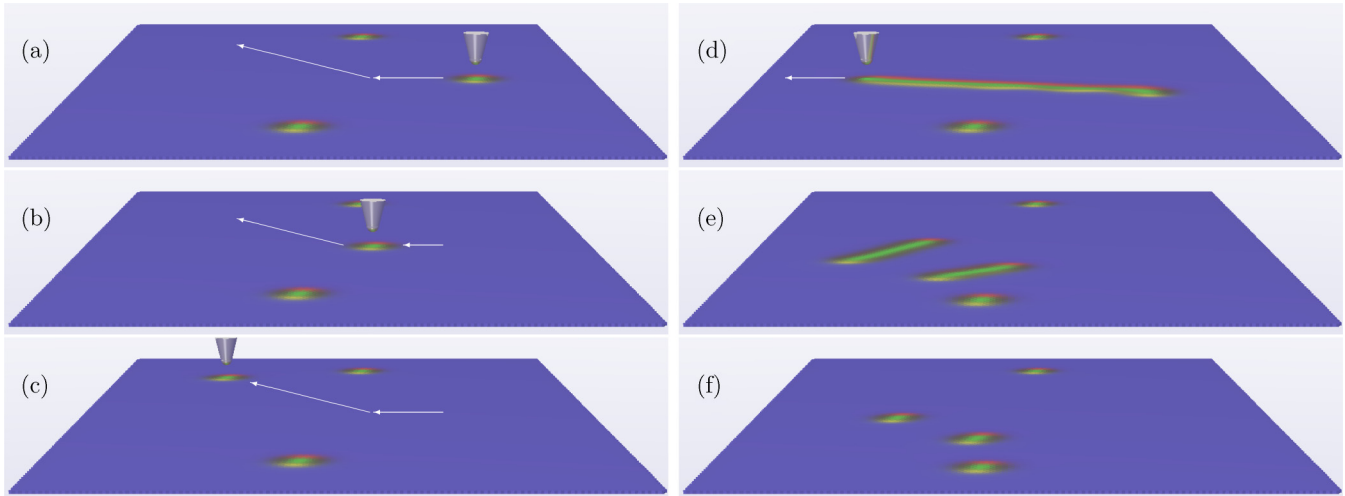


FIG. 3. Manipulation of a single Skyrmion with a spin-polarized STM. Left column: Slow velocity and moderate current strength. Right column: Fast velocity and high current.

the surrounding skyrmions can be seen. The energy win just for the central spin can be easily calculated. In the case of a collinear structure and under the assumption of the Hamiltonian  $\mathcal{H}$  a reversed central spin with six nearest neighbors will set free an energy of  $\Delta E = 6J + 2\mu_S B_z$ .

Besides the creation and annihilation of skyrmions the scanning tunneling microscope can be also used to move skyrmions. The possibility to shift domain walls has been discussed in [21,26]. Figure 3(a) shows a sequence of pictures where the movement of a single skyrmion with a moving scanning tunneling tip is demonstrated. The tip has a polarization in  $-z$  direction which is opposite to the orientation of the ferromagnetic surrounding the skyrmion but parallel to the orientation in the center. In former publications it has been shown that a tip polarization parallel to the magnetization in the center of the domain wall is the best choice. In the case of the skyrmion a tip polarization parallel to the central magnetization is the best decision and has been used during the simulations. In this case,  $I_0 = 2.0 \times 10^{17}$  1/s has been assumed. During the simulations faster velocities than the 5.5 nm/s of a conventional STM tip have been used to finish the calculations in an adequate time. However, as long as the tip velocity is smaller than the maximal possible velocity of the magnetic skyrmion [27] the skyrmion will be captured by the STM tip and moves with the same velocity as the tip. If the tip moves faster than the maximal possible skyrmion velocity the STM tip will lose the magnetic skyrmion. What happens if the tip moves too fast can be seen in Figs. 3(d)–3(f). Here a larger current intensity ( $I_0 = 2.0 \times 10^{19}$  1/s) and a tip velocity of 1080 m/s have been assumed. In this case the current creates a Bimeron [28,29] which is not stable. The Bimeron collapses into several shorter Bimerons which become under rotational movements magnetic skyrmions. A similar scenario has been recently reported for heavy metal/thin ferromagnet/insulator trilayer structures after applying current pulses [10].

Until now the skyrmion has been manipulated with aid of a spin-polarized tunnel current. However, using spin-polarized current means that it is needed to have a stable spin-polarized

tip. Furthermore, for the spatial manipulation of the magnetic skyrmion (see Fig. 3) a tip polarization is needed which is opposite to the external field. Due to these conditions it is more effective if the manipulation could be done with an unpolarized tip. Recently Hsu *et al.* [16] have shown that it is possible to create and annihilate skyrmions by using electric field pulses (Figs. 4 and 5). The performed simulations show that all the scenarios presented before: moving, creating, and annihilating of skyrmions, can be done with an electric field. The electric field itself is local and affects locally the DMI [30,31]:

$$\mathcal{D}_{nm} = \mathcal{D}_{nm}^0 + \omega_{nm}(\mathbf{E} \times \mathbf{r}_{nm}).$$

$\mathcal{D}_{nm}^0$  is the original DMI without electric field,  $\mathbf{E}$  is the electric field vector,  $\mathbf{r}_{nm} = \mathbf{r}_n - \mathbf{r}_m$  is the vector pointing from lattice site  $n$  to lattice site  $m$ , and  $\omega_{nm}$  is a constant. If, as in the experiment, the electric field is given by a vector pointing in  $\pm z$  direction (perpendicular to the film plane)  $\mathbf{E} \times \mathbf{r}_{nm}$  will be parallel/antiparallel to the DMI vector and increases or decreases the effect of the DMI. This means especially if the electric field is oriented in such a way that it neglects the DMI the skyrmion gets annihilated. Without DMI the ferromagnetic configuration is the ground state and the magnetic field which has stabilized the skyrmion destroys it now. During the simulation of the annihilation process using an electric field the DMI underneath the STM tip has been reduced using a Gaussian similar to the one used for the electric current (Terstoff-Haman model) added to the original

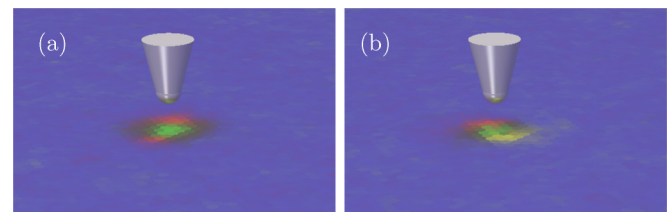


FIG. 4. Skyrmion creation with (a) spin-polarized current and (b) with electric field: configurations shortly after the process has started.

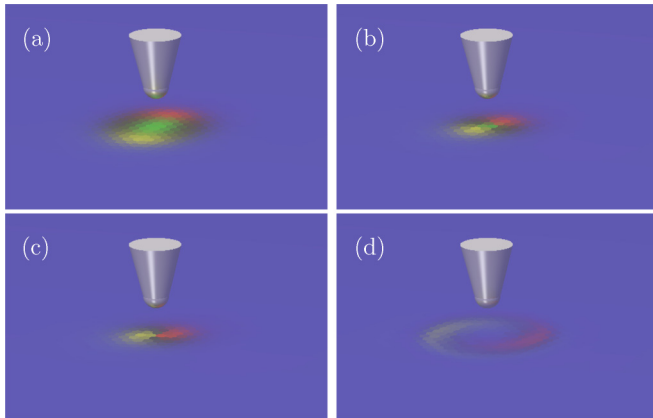


FIG. 5. Annihilation of the magnetic skyrmion (a) with an electric field. Three phases: (b) shrinking, (c) core collapse, and (d) shock wave.

DMI and with the boundary condition that the DMI does not become negative (negative values have been set equal to zero). The assumed values are  $I_0 = -42 \times 10^3$  meV,  $\kappa = 3.5$ , and  $P = -1$ . The modification was switched on at the beginning of the simulation and suddenly switched off after 50 ps. The dynamics in this case is similar to the one described in [18,32]. Three phases can be observed: first the reduction of the skyrmion size and then the reversal of the center of the skyrmion (second phase). During this reversal process the skyrmion releases energy which can be seen in the form of a concentric shockwave running through the system (third phase). During the first phase (reduction of the radius) the skyrmion shows a twist of the magnetic moments which ends with the annihilation of the skyrmion. The creation process of the magnetic skyrmion is a little bit more complex. Here the electric field strengthens the DMI. During the simulation the DMI underneath the STM tip has been increased. Here the same Gaussian as before, just with  $P = +1$ , and the same time

modification have been used. However, this is not enough to create the skyrmion. To create the skyrmion first the symmetry of the ferromagnetic order needs to be broken. In other words, first a region of opposite magnetization has to be created which becomes the center of the skyrmion. Here temperature fluctuations help. Koshibae and Nagaosa have shown that a locally increased temperature can be used to create a skyrmion [33]. Another ingredient which can help to create the skyrmion, but has not been used during the simulations, is the fact that electric field not only changes the strength of the DMI, but also the strength of uniaxial anisotropies [34,35].

To move the skyrmion an electric field with the same field direction as used for the creation of the skyrmion (in the case of Hsu *et al.* [16] pointing away from the film plane) can be used. Here the electric field increases the DMI and therefore decreases the energy of the skyrmion. The movement of the STM tip with adequate velocity lets the skyrmion follow. Thereby the dynamics is the same as using a spin-polarized tunnel current.

In summary, computer simulations of a magnetic skyrmion in an atomic spin system with a triangular lattice have been performed. It has been shown that it is possible to use a scanning tunneling microscope to manipulate: create, annihilate, and move a single skyrmion, either by a spin-polarized current or an electric field. The creation and annihilation of the skyrmion reproduces the results of the experiments. However, the time average of a conventional STM is too low to see the dynamics during these events. The performed simulations deliver the missing information and give an explanation for the underlying physics. The aimed motion of the skyrmion has not been demonstrated in experiments so far but the performed simulations show the possibility. Although the given description is with Pd/Fe/Ir(111) for magnetic skyrmions on the atomic length scale the relevance is not restricted. In the case of magnetic skyrmions with diameters up to  $\sim 90$  nm as for  $\text{Fe}_{0.5}\text{Co}_{0.5}\text{Si}$  [36] the STM tip can be seen as a synonym for an electrode of a few micro- or millimeters.

- 
- [1] X. Zhang *et al.*, *Sci. Rep.* **5**, 7643 (2015).  
 [2] Y. Zhou and M. Ezawa, *Nat. Commun.* **5**, 4652 (2014).  
 [3] A. Fert, V. Cros, and J. Sampaio, *Nat. Nanotech.* **8**, 152 (2013).  
 [4] X. Zhang, M. Ezawa, and Y. Zhou, *Sci. Rep.* **5**, 9400 (2015).  
 [5] X. Zhang *et al.*, *Sci. Rep.* **5**, 11369 (2015).  
 [6] T. H. O'Dell, *Rep. Prog. Phys.* **49**, 589 (1986).  
 [7] S. S. P. Parkin, M. Hayashi, and L. Thomas, *Science* **320**, 190 (2008).  
 [8] R. Wieser, K. D. Usadel, and U. Nowak, *Phys. Rev. B* **74**, 094410 (2006).  
 [9] K. Yamada *et al.*, *Nat. Mater.* **6**, 270 (2007).  
 [10] W. Jiang *et al.*, *Science* **349**, 283 (2015).  
 [11] S. Woo *et al.*, *Nat. Mater.* **15**, 501 (2016).  
 [12] S. Mühlbauer *et al.*, *Science* **323**, 915 (2009).  
 [13] N. Romming *et al.*, *Science* **341**, 636 (2013).  
 [14] J. Barker and O. A. Tretiakov, *Phys. Rev. Lett.* **116**, 147203 (2016).  
 [15] S.-Z. Lin, *Phys. Rev. B* **94**, 020402(R) (2016).  
 [16] P.-J. Hsu *et al.*, *Nat. Nano.*, doi: 10.1038/nnano.2016.234 (2016).  
 [17] J. Hagemester *et al.*, *Nat. Commun.* **6**, 8455 (2015).  
 [18] A. Siemens *et al.*, *New J. Phys.* **18**, 045021 (2016).  
 [19] See Supplemental Material at <http://link.aps.org/supplemental/10.1103/PhysRevB.95.064417> for a full list and description of the attached movies, remarks concerning simulations with and without temperature and simulations with and without uniaxial anisotropy, and additional information about the computer program used.  
 [20] J. Tersoff and D. R. Hamann, *Phys. Rev. Lett.* **50**, 1998 (1983).  
 [21] T. Stapelfeldt, R. Wieser, E. Y. Vedmedenko, and R. Wiesendanger, *Phys. Rev. Lett.* **107**, 027203 (2011).  
 [22] H.-B. Braun, *Adv. Phys.* **61**, 1 (2012).  
 [23] Y. Onose, Y. Okamura, S. Seki, S. Ishiwata, and Y. Tokura, *Phys. Rev. Lett.* **109**, 037603 (2012).  
 [24] J. V. Kim, F. Garcia-Sanchez, J. Sampaio, C. Moreau-Luchaire, V. Cros, and A. Fert, *Phys. Rev. B* **90**, 064410 (2014).

- [25] Y. Liu, H. Du, M. Jia, and A. Du, *Phys. Rev. B* **91**, 094425 (2015).
- [26] R. Wieser *et al.*, *Europhys. Lett.* **97**, 17009 (2012).
- [27] J. Iwasaki, M. Mochizuki, and N. Nagaosa, *Nat. Commun.* **4**, 1463 (2013).
- [28] M. Ezawa, *Phys. Rev. B* **83**, 100408(R) (2011).
- [29] H. Du, W. Ning, M. Tian, and Y. Zhang, *Phys. Rev. B* **87**, 014401 (2013).
- [30] K. Siratori and E. Kita, *J. Phys. Soc. Jpn.* **48**, 1443 (1980).
- [31] W. Chen and M. Sigrist, *Phys. Rev. Lett.* **114**, 157203 (2015).
- [32] R. Wieser, [arXiv:1610.03191](https://arxiv.org/abs/1610.03191).
- [33] W. Koshibae and N. Nagaosa, *Nat. Commun.* **5**, 5148 (2014).
- [34] W. J. Zhou *et al.*, *Sci. Rep.* **4**, 4117 (2014).
- [35] Y. Hibino *et al.*, *Appl. Phys. Express* **8**, 113002 (2015).
- [36] X. Z. Yu *et al.*, *Nature (London)* **465**, 901 (2010).